The Astrophysical Journal, 692:L130–L133, 2009 February 20 doi:10.1088/0004-637X/692/2/L130

EVOLUTION OF THE COSMIC-RAY ANISOTROPY ABOVE 10^{14} eV

M. Aglietta[1,2], V. V. Alekseenko[3], B. Alessandro[2], P. Antonioli[4], F. Arneodo[5], L. Bergamasco[2,6], M. Bertaina[2,6], R. Bonino[1,2], A. Castellina[1,2], A. Chiavassa[2,6], B. D'Ettorre Piazzoli[7], G. Di Sciascio[7,8], W. Fulgione[1,2], P. Galeotti[2,6], P. L. Ghia[1,5,9], M. Iacovacci[7], G. Mannocchi[1,2], C. Morello[1,2], G. Navarra[2,6], O. Saavedra[2,6], A. Stamerra[6,10], G. C. Trinchero[1,2], S. Valchierotti[2,6], P. Vallania[1,2], S. Vernetto[1,2], C. Vigorito[2,6], and

The EAS-TOP Collaboration

[1] Istituto di Fisica dello Spazio Interplanetario, INAF, Torino, Italy
[2] Istituto Nazionale di Fisica Nucleare, Torino, Italy
[3] Institute for Nuclear Research, AS Russia, Baksan Neutrino Observatory, Russia
[4] Istituto Nazionale di Fisica Nucleare, Bologna, Italy
[5] Laboratori Nazionali del Gran Sasso, INFN, Assergi (AQ), Italy
[6] Dipartimento di Fisica Generale dell'Università, Torino, Italy
[7] Dipartimento di Scienze Fisiche dell'Università, INFN, Napoli, Italy
Received 2008 December 2; accepted 2009 January 14; published 2009 February 6

ABSTRACT

The amplitude and phase of the cosmic-ray anisotropy are well established experimentally between 10^{11} eV and 10^{14} eV. The study of their evolution in the energy region 10^{14}–10^{16} eV can provide a significant tool for the understanding of the steepening ("knee") of the primary spectrum. In this Letter, we extend the EAS-TOP measurement performed at $E_0 \approx 10^{14}$ eV to higher energies by using the full data set (eight years of data taking). Results derived at about 10^{14} and 4×10^{14} eV are compared and discussed. Hints of increasing amplitude and change of phase above 10^{14} eV are reported. The significance of the observation for the understanding of cosmic-ray propagation is discussed.

Key words: cosmic rays – diffusion

1. INTRODUCTION

The steepening ("knee") observed at $E_0 \approx 3 \times 10^{15}$ eV represents a main feature of the energy spectrum of cosmic rays and its characterization is therefore a main tool for the understanding of the galactic radiation. Composition studies have shown that it is related to the steepening of the spectra of the lightest primaries (protons, helium, CNO: Aglietta et al. 2004; Antoni et al. 2005).

Such an effect can be due, on the one hand, to energy limits of the acceleration process at the source, namely diffusive shock acceleration in supernova remnants, generally considered to be the sources of galactic cosmic rays. The maximum energy of the accelerated protons is, indeed, calculated to occur in the 10^{15} eV energy region (Berezhko et al. 1996; Berezhko & Volk 2007), but could reach up to about 10^{17} eV (Ptuskin & Zirakashvili 2003). On the other hand, this feature has been possibly explained in terms of a change in the cosmic-ray propagation properties inside the Galaxy (Peters 1960; Zatsepin et al. 1962). Galactic propagation is described through diffusion models whose parameters have been obtained through composition studies (mainly from the ratio of secondary to primary nuclei) at energies well below 10^{12} eV (see, e.g., Jones et al. 2001; Strong et al. 2007). The diffusion coefficient, D, is found to increase with magnetic rigidity ($D \propto R^{0.6}$, or $D \propto R^{0.3}$ for models including reacceleration). However, no confirmation, and no information, has till now been obtained at higher energies, where the main observable is represented by the large-scale anisotropy in the cosmic rays' arrival directions that is known to be strictly related to the diffusion coefficient (see, e.g., Berezinsky et al. 1990). The study of the evolution of the anisotropy in the "knee" energy region can therefore provide a significant test of the diffusion models and a valuable insight into the discrimination between the two possible explanations of the spectral steepening.

At $E_0 \approx 10^{14}$ eV, the EAS-TOP[11] results (Aglietta et al. 1996) demonstrated that the main features of the anisotropy (i.e., of cosmic-ray propagation) are similar to those measured at lower energies (10^{11}–10^{14} eV), both with respect to amplitude ($(3\text{–}6) \times 10^{-4}$) and phase ((0–4) hr local sidereal time (LST)) (Gombosi et al. 1975; Fenton et al. 1975; Nagashima et al. 1989; Alekseenko et al. 1981; Andreev et al. 1987; Ambrosio et al. 2003; Munakata et al. 1997; Amenomori et al. 2005; Guillian et al. 2007; Abdo et al. 2008). At higher energies the limited statistics do not allow any firm conclusion to be drawn (Kifune et al. 1984; Gherardy et al. 1983; Antoni et al. 2004; Amenomori et al. 2006; Over et al. 2007).

In this Letter, we present the EAS-TOP measurement based on the full data set and we extend the analysis to about 4×10^{14} eV.

2. THE EXPERIMENT AND THE ANALYSIS

The EAS-TOP Extensive Air Shower array was located at Campo Imperatore (2005 m a.s.l., latitude 42°27′N, longitude 13°34′E, INFN Gran Sasso National Laboratory). The electromagnetic detector used for the present analysis (Aglietta et al. 1993) consisted of 35 modules of scintillator counters, 10 m^2 each, distributed over an area of about 10^5 m^2. The trigger was provided by the coincidence of any four neighboring modules (threshold $n_p \approx 0.3$ minimum ionizing particles per module), the event rate being $f \approx 25$ Hz. The data under discussion have

[8] Presently at Istituto Nazionale di Fisica Nucleare, Roma Tor Vergata, Italy.
[9] Presently at Institut de Physique Nucléaire, CNRS, Orsay, France.
[10] Presently at Dipartimento di Fisica dell'Università and INFN, Pisa, Italy.

[11] The Extensive Air Shower array on TOP of the Gran Sasso underground laboratories.

Table 1
Characteristics of the Two Classes of Events Used in the Analysis

Class	$N_{\rm modules}$[a]	E_0 (eV)[b]	$N_{\rm EW}$[c]
I	$\geqslant 4$	1.1×10^{14}	1.5×10^{9}
II	$\geqslant 12$	3.7×10^{14}	1.7×10^{8}

Notes.
[a] Number of triggered modules; [b] primary energy; and [c] number of collected events in the east + west sectors.

been collected between 1992 January and 1999 December for a total of 1431 full days of operation.

To select different primary energies, a cut is applied to the events based on the number of triggered modules (see Table 1). The average primary energies are evaluated for primary protons and the QGSJET01 hadron interaction model (Kalmykov et al. 1997) in CORSIKA (Heck et al. 1998).

For the analysis of the anisotropy, we adopt a method based on the counting rate differences between eastward and westward directions, which allows us to remove counting rate variations of atmospheric origin. The events used in the analysis (see Table 1) are those with the azimuth angle ϕ inside $\pm 45^\circ$ around the east and west directions, and the zenith angle $\theta < 40^\circ$. The difference between the number of counts measured from the east sector, $C_E(t)$, and from the west one, $C_W(t)$, at time t in a fixed interval ($\Delta t = 20$ minutes), is related to the first derivative of the intensity $I(t)$ as $\frac{dI}{dt} \simeq D(t) = \frac{C_E(t) - C_W(t)}{\delta t}$, where δt is the average hour angle between the vertical and each of the two sectors (1.7 hr in our case). The harmonic analysis is performed on the differences $D(t)$; the amplitudes and phases of the variation of $I(t)$ are obtained through the integration of the corresponding terms of the Fourier series (Aglietta et al. 2007).

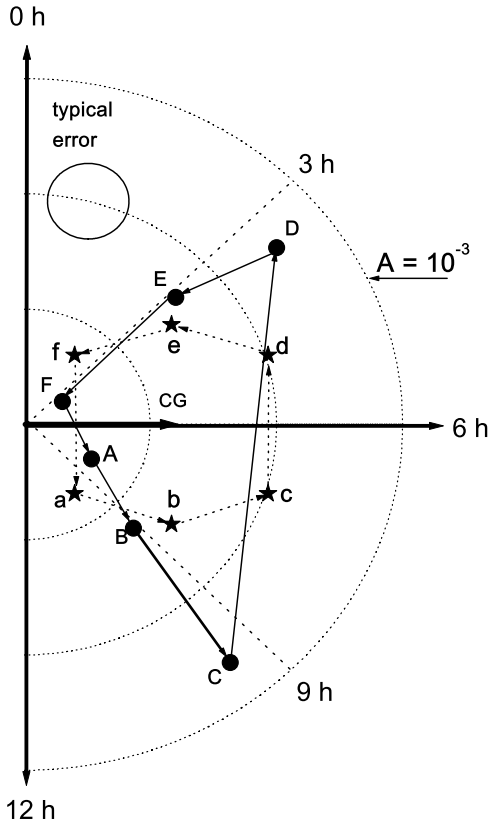

Figure 1. Bimonthly solar vectors at 1.1×10^{14} eV. Capital and lower-case refer respectively to the expected and theoretical points (A, a = January + February; B, b = March + April; C, c = May + June; D, d = July + August; E, e = September + October; F, f = November + December). The typical vector statistical uncertainty is shown.

3. RESULTS

The harmonic analysis has been performed in solar, sidereal, and antisidereal time.[12] We describe in Section 3.1 the results of the analysis, while in Section 3.2 we show the related counting rate curves.

3.1. The Harmonic Analysis

For the two different primary energies, the reconstructed amplitudes and phases of the first and second harmonics are shown in Table 2 together with the corresponding Rayleigh imitation probabilities (P).

Concerning the *first harmonic*:

1. At 1.1×10^{14} eV, from the analysis in solar time, the obtained amplitude and phase $\left(A^I_{\rm sol} = (2.8 \pm 0.8) \times 10^{-4}, \phi^I_{\rm sol} = (6.0 \pm 1.1)\ \text{hr}, P^I_{\rm sol} = 0.2\%\right)$ are in excellent agreement with the expected ones from the Compton–Getting effect (Compton & Getting 1935) due to the revolution of the Earth around the Sun: at our latitude $A_{\rm sol,CG} = 3.0 \times 10^{-4}$, $\phi_{\rm sol,CG} = 6.0$ hr.

   With respect to the sidereal time analysis, the measured amplitude and phase $\left(A^I_{\rm sid} = (2.6 \pm 0.8) \times 10^{-4}, \phi^I_{\rm sid} = (0.4 \pm 1.2)\ \text{hr LST}\right)$, with imitation probability $P^I_{\rm sid} = 0.5\%$, confirm the previous EAS-TOP result (Aglietta et al. 1996).

   Bimonthly vectors representing the first harmonic are shown in Figure 1 (dots), together with the expected ones (stars) from the measured solar and sidereal amplitudes. The expected counterclockwise rotation of the vector is clearly visible, showing that, at any time, the composition of the two vectors is observed, and that the expected and measured individual values are fully compatible within the statistical uncertainties.

2. At 3.7×10^{14} eV the amplitude and phase of the measured first harmonic in solar time are still consistent with the expected ones for the solar Compton–Getting effect, although, due to the reduced statistics, the chance imitation probability is rather high.

   Concerning the analysis in sidereal time, we obtain $A^I_{\rm sid} = (6.4 \pm 2.5) \times 10^{-4}$, $\phi^I_{\rm sid} = (13.6 \pm 1.5)$ hr LST, with an imitation probability of about 3.8%. This indicates, therefore, a change of phase (from 0.4 to 13.6 hr) and an increase of amplitude (by a factor of 2.5) with respect to the first harmonic measured at 1.1×10^{14} eV.

Concerning the *second harmonic*: most significant $\left(P^{II}_{\rm sid} = 1.6\%\right)$ is the amplitude observed in sidereal time in the lower-energy class of events (comparable with the first harmonic one: $A^{II}_{\rm sid} = (2.3 \pm 0.8) \times 10^{-4}$, $\phi^{II}_{\rm sid} = (6.3 \pm 0.7)$ hr LST; see also Alekseenko et al. 1981).

Both at 1.1×10^{14} eV and 3.7×10^{14} eV, no significant amplitude is observed in antisidereal time, showing that no additional correction is required due to residual seasonal effects.

[12] The antisidereal time is a fictitious timescale symmetrical to the sidereal one with respect to the solar time and that reflects seasonal influences (Farley & Storey 1954).

Table 2
Results of the Analysis of the First (Amplitude $A^{\rm I}$, Phase $\phi^{\rm I}$, and Rayleigh Imitation Probability $P^{\rm I}$) and Second Harmonic ($A^{\rm II}$, $\phi^{\rm II}$, $P^{\rm II}$) in Solar (Columns 2–4), Sidereal (Columns 5–7), and Antisidereal Time (Columns 8–10)

E_0 (eV)	$A^{\rm I}_{\rm sol}10^4$	$\phi^{\rm I}_{\rm sol}$ (hr)	$P^{\rm I}_{\rm sol}$ (%)	$A^{\rm I}_{\rm sid}10^4$	$\phi^{\rm I}_{\rm sid}$ (hr)	$P^{\rm I}_{\rm sid}$ (%)	$A^{\rm I}_{\rm asid}10^4$	$\phi^{\rm I}_{\rm asid}$ (hr)	$P^{\rm I}_{\rm asid}$ (%)
1.1×10^{14}	2.8 ± 0.8	6.0 ± 1.1	0.2	2.6 ± 0.8	0.4 ± 1.2	0.5	1.2 ± 0.8	23.9 ± 2.8	32.5
3.7×10^{14}	3.2 ± 2.5	6.0 ± 3.4	44.1	6.4 ± 2.5	13.6 ± 1.5	3.8	3.4 ± 2.5	22.3 ± 3.2	39.7
	$A^{\rm II}_{\rm sol}10^4$	$\phi^{\rm II}_{\rm sol}$ (hr)	$P^{\rm II}_{\rm sol}$ (%)	$A^{\rm II}_{\rm sid}10^4$	$\phi^{\rm II}_{\rm sid}$ (hr)	$P^{\rm II}_{\rm sid}$ (%)	$A^{\rm II}_{\rm asid}10^4$	$\phi^{\rm II}_{\rm asid}$ (hr)	$P^{\rm II}_{\rm asid}$ (%)
1.1×10^{14}	1.4 ± 0.8	7.0 ± 1.2	21.6	2.3 ± 0.8	6.3 ± 0.7	1.6	0.6 ± 0.8	...	75.5
3.7×10^{14}	1.7 ± 2.5	...	79.4	1.5 ± 2.5	...	83.5	1.2 ± 2.5	...	89.1

Note. Phases are not defined when amplitudes are smaller than their uncertainties.

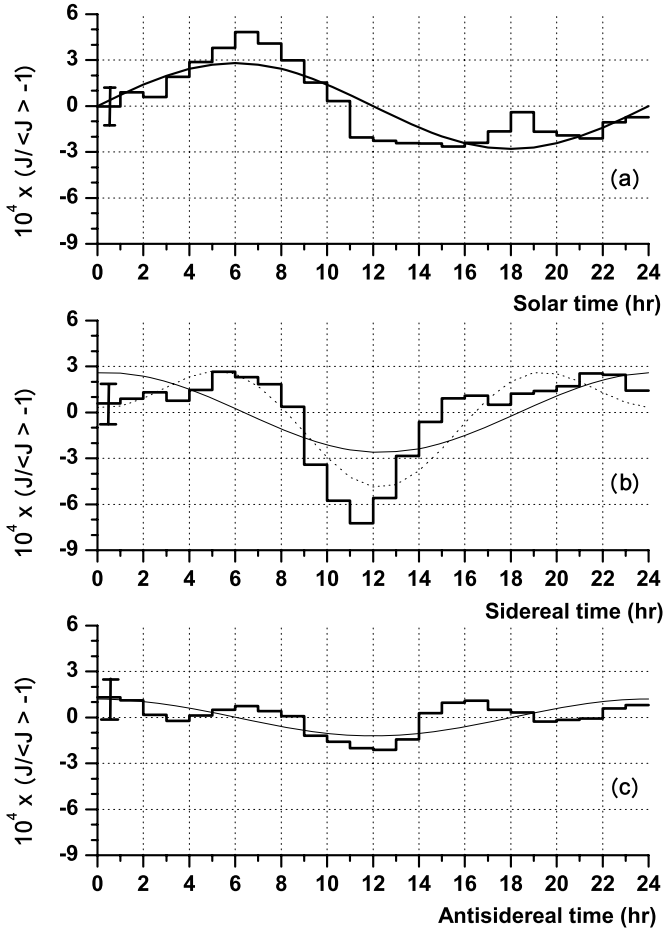

Figure 2. Thick black lines: counting rate curves in solar (a), sidereal (b), and antisidereal (c) time at 1.1×10^{14} eV. The statistical uncertainty for each bin is given in the first one. The curves resulting from the first harmonic analysis are also shown (light black lines); for the sidereal time curve, the combination of the first and second harmonics (dotted black line) is additionally superimposed.

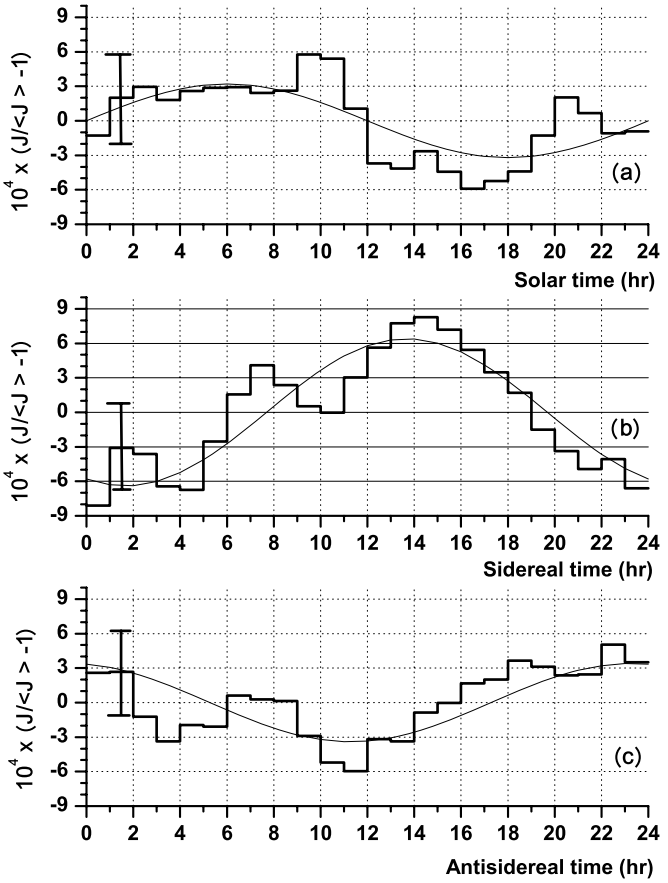

Figure 3. Thick black lines: counting rate curves in solar (a), sidereal (b), and antisidereal (c) time at 3.7×10^{14} eV. The curves resulting from the first harmonic analysis are also shown (light black lines).

3.2. The Counting Rate Curves

Besides the harmonic analysis, it is interesting to visualize the variations of the cosmic-ray intensity versus time, $I(t)$, as reconstructed by the integration of the east–west differences, $D(t)$. They are shown in Figures 2 and 3 for the classes of events at 1.1×10^{14} eV and 3.7×10^{14} eV, respectively (a, b, and c for solar, sidereal, and antisidereal timescales).

As already shown by the harmonic analysis, at both energies the curves in solar time are dominated by the Compton–Getting effect due to the motion of the Earth, and no modulation is visible in the antisidereal timescale.

A main difference is observed in the sidereal time curves: while the shape of the curve at 1.1×10^{14} eV is in remarkable agreement with the EAS and muon measurements reported at and below 10^{14} eV, the curve related to the highest energy class of events is characterized by a broad excess around 13–16 hr LST.

4. CONCLUSIONS

High-stability data obtained from long-time observations (eight years) from the EAS-TOP array confirm the amplitude and phase of the cosmic-ray anisotropy already reported at 10^{14} eV: $A^I_{\rm sid} = (2.6 \pm 0.8) \times 10^{-4}$, $\phi^I_{\rm sid} = (0.4 \pm 1.2)$ hr LST, with the Rayleigh imitation probability $P^I_{\rm sid} = 0.5\%$. The result is supported by the observation of the Compton–Getting effect due to the revolution of the Earth around the Sun, and by the absence of antisidereal effects. It confirms the homogeneity of the anisotropy data over the energy range 10^{11}–10^{14} eV.

At higher energies (around 4×10^{14} eV) the observed anisotropy shows a larger amplitude, $A^I_{\rm sid} = (6.4 \pm 2.5) \times 10^{-4}$, and a different phase, $\phi^I_{\rm sid} = (13.6 \pm 1.5)$ hr LST, with an imitation probability of 3.8%. The statistical significance is still limited, but the measurement has the highest sensitivity with respect to previous experiments at these energies, and it is not in contradiction with any of them.

The dependence of the anisotropy amplitude over primary energy $\left(A \propto E_0^{\delta}\right)$ deduced from the present two measurements can be represented by a value of $\delta = 0.74 \pm 0.41$. Therefore, at least in the energy range $(1 - 4) \times 10^{14}$ eV, such dependence is compatible with that of the diffusion coefficient as derived by composition measurements at lower energies.

On the other hand, the sharp increase of the anisotropy above 10^{14} eV may be indicative of a sharp evolution of the propagation properties, and therefore of the diffusion coefficient just approaching the steepening of the primary spectrum. This opens the problems of obtaining an improved theoretical and experimental description of the whole evolution of the diffusion processes versus primary energy, and understanding how such evolution could affect the energy spectra at the "knee." From the experimental point of view, the extension of the anisotropy measurements with high sensitivity to and above 10^{15} eV will be of crucial significance.

V.V.A. is grateful to the INFN Gran Sasso National Laboratory for financial support through FAI funds. P.L.G. acknowledges the financial support by the European Community 7th Framework Program through the Marie Curie Grant PIEF-GA-2008-220240.

REFERENCES

Abdo, A. A., et al. 2008, arXiv:0806.2293
Aglietta, M., et al. 1993, Nucl. Instrum. Methods Phys. Res. A., 336, 310
Aglietta, M., et al. 1996, ApJ, 470, 501
Aglietta, M., et al. 2004, Astropart. Phys., 21, 583
Aglietta, M., et al. 2007, in Proc. 30th ICRC, ed. R. Caballero, et al., 4, 51
Alekseenko, V. V., et al. 1981, in Proc. 17th ICRC, ed. Commissariat à l'Energie Atomique, 2, 146
Ambrosio, M., et al. 2003, Phys. Rev. D, 67, 042002
Amenomori, M., et al. 2005, ApJ, 626, L29
Amenomori, M., et al. 2006, Science, 314, 439
Andreev, Y., et al. 1987, Proc. 20th ICRC, ed. V. A. Kozyarivksy, 2, 22
Antoni, T., et al. 2004, ApJ, 604, 687
Antoni, T., et al. 2005, Astropart. Phys., 24, 1
Berezhko, E. G., & Volk, H. J. 2007, ApJ, 661, L175
Berezhko, E. G., et al. 1996, J. Exp. Theor. Phys., 82, 1
Berezinsky, V., et al. 1990, in Astrophysics of Cosmic Rays, ed. V. L. Ginzburg (Amsterdam: North Holland)
Compton, A. H., & Getting, I. A. 1935, Phys. Rev., 47, 817
Farley, F. J. M., & Storey, J. R. 1954, Proc. Phys. Soc., 67, 996
Fenton, B. K., et al. , et al. 1975, in Proc. 14th ICRC, ed. K. Pinkau, et al., 4, 1482
Gherardy, P., et al. 1983, J. Phys. G, 9, 1279
Gombosi, T., et al. 1975, Nature, 255, 687
Guillian, G., et al. 2007, Phys. Rev. D, 75, 062003
Heck, D., et al. 1998, FZK Report, 6019
Jones, F. C., et al. 2001, ApJ, 547, 264
Kalmykov, N. N., et al. 1997, Nucl. Phys. B, 52, 17
Kifune, T., et al. 1984, J. Phys. G, 12, 129
Munakata, K., et al. 1997, Phys. Rev. D, 56, 23
Nagashima, K., et al. 1989, Nuovo Cimento C, 12, 695
Over, S., et al. , et al. 2007, in Proc. 30th ICRC, ed. R. Caballero, et al., 4, 223
Peters, P. 1960, in Proc. 6th ICRC, ed. L. I. Dorman & V. F. Tulinov, 3, 157
Ptuskin, V. S., & Zirakashvili, V. N. 2003, A&A, 403, 1
Strong, A. W., et al. 2007, Annu. Rev. Nucl. Part. Sci., 50, 1, 285
Zatsepin, G. T., et al. 1962, Izv. Akad. Nauk USSR S. P., 26, 685